

Turbulence and the formation of filaments, loops and shock fronts in NGC 1275

D Falceta-Gonçalves¹, E M de Gouveia Dal Pino², J S Gallagher³ & A Lazarian³

1 - Núcleo de Astrofísica Teórica, Universidade Cruzeiro do Sul - Rua Galvão Bueno 868, CEP 01506-000, São Paulo, Brazil;

2 - Instituto de Astronomia, Geofísica e Ciências Atmosféricas, Universidade de São Paulo, Rua do Matão 1226, CEP 05508-900, São Paulo, Brazil;

3 - Astronomy Department, University of Wisconsin, Madison, 475 N. Charter St., WI 53711, USA

E-mail: diego.goncalves@cruzeirodosul.edu.br, dalpino@astro.iag.usp.br, jsg@facstaff.wisc.edu, alazarian@sfacstaff.wisc.edu

Abstract. NGC 1275, the central galaxy in the Perseus cluster, is the host of gigantic hot bipolar bubbles inflated by AGN jets observed in the radio as Perseus A. It presents a spectacular $H\alpha$ -emitting nebulosity surrounding NGC 1275, with loops and filaments of gas extending to over 50 kpc. The origin of the filaments is still unknown, but probably correlates with the mechanism responsible for the giant buoyant bubbles. We present 2.5 and 3-dimensional MHD simulations of the central region of the cluster in which turbulent energy, possibly triggered by star formation and supernovae (SNe) explosions is introduced. The simulations reveal that the turbulence injected by massive stars could be responsible for the nearly isotropic distribution of filaments and loops that drag magnetic fields upward as indicated by recent observations. Weak shell-like shock fronts propagating into the ICM with velocities of 100-500 km/s are found, also resembling the observations. The isotropic outflow momentum of the turbulence slows the infall of the intracluster medium, thus limiting further starburst activity in NGC 1275. As the turbulence is subsonic over most of the simulated volume, the turbulent kinetic energy is not efficiently converted into heat and additional heating is required to suppress the cooling flow at the core of the cluster. Simulations combining the MHD turbulence with the AGN outflow can reproduce the temperature radial profile observed around NGC 1275. While the AGN mechanism is the main heating source, the supernovae are crucial to *isotropize* the energy distribution.

PACS numbers: 98.65.-r, 98.65.Hb, 02.60.Cb

1. Introduction

Perseus (Abell 426) at $z = 0.0176$ is the brightest galaxy cluster in X-ray, is a *prototype* of cooling core clusters. Its central galaxy, NGC 1275, hosts a narrow-line radio source, Per A (3C84), which interacts with the intracluster gas through its jets and bipolar outflows. *Chandra* X-ray observations (Fabian et al. 2003, 2006, Saunders & Fabian 2007) reveal an associated complex intracluster medium (ICM), with temperatures ranging from 2.5 keV near NGC 1275 up to 7 keV in the outskirts. Features like X-ray cavities and spherical shock waves (Graham, Fabian & Sanders 2008) observed in its thermal plasma seem to be associated with energy flows in the central region.

A rich filamentary structure of cold gas is roughly isotropically distributed around NGC 1275 ($\sim 1 - 10^3 \text{ cm}^{-3}$ and $T \sim 10^3 - 10^4 \text{ K}$) (Conselice, Gallagher & Wise 2001, Salome et al. 2006, Fabian et al. 2003, Fabian et al. 2008). It extends to $\sim 75 \text{ kpc}$ in radius and is $> 10^8 \text{ yr}$ old, and its origin is still undetermined (Johnstone et al 2007, Ferland et al. 2008, Revaz et al. 2008). The filaments have radial velocities of $\sim 200 \text{ km s}^{-1}$, much smaller than the sound speed of $\sim 700 \text{ km s}^{-1}$ in the surrounding hot ICM (Hatch et al. 2006, Gallagher et al. in preparation). The mechanism by which the filaments are stabilized against disruption into the pervasive $4 \times 10^7 \text{ K}$ ICM is also unclear, but a magnetic field in the filaments ($\sim 100 \mu\text{G}$) in equipartition with the surrounding pressure would be sufficient to assure their stabilization (Fabian et al. 2008).

It has been suggested that the formation of filaments and the increase of turbulent energy in galaxy clusters could be related to the cooling flows and the consequent magnetic compression (Pistinner & Shaviv 1995, Godon et al. 1998). However, there is no evidence of strong cooling flows that could reproduce these models. Both the origins of the giant gas filaments and suppression of the cooling flow in A426 can be associated with the presence of giant bubbles of hot gas inflated by the AGN (Fabian et al. 2003). However, recent hydrodynamical simulations have shown that the AGN feedback seems to be insufficient to reduce the cooling flow effects to the observed values, $T_{\text{ICM}}/T_{\text{core}} \sim 3$ (Gardini 2007). Simulations also suggest that AGN are likely to be ineffective in creating a nearly isotropic distribution of filaments. This is because, despite the large AGN power output ($10^{42} - 10^{44} \text{ erg s}^{-1}$), which explains the production of the hot bubbles, the low density and momentum associated with the relativistic jets do not readily distribute the thermal energy isotropically. Additional energy/momentum mechanism(s) may be required to produce both the isotropic filamentary structure and the isotropization of energy.

The issue of AGN feedback in galaxy clusters presents a number of unsolved problems yet which have been extensively discussed in the literature. Besides those discussed above, hydrodynamical simulations have also shown that the AGN bubbles may disrupt within 100 Myr due to Kelvin-Helmholtz and Rayleigh-Taylor instabilities (Bruggen et al. 2005, Heinz et al. 2006, Pizzolato & Soker 2006), failing to reproduce the observed ICM cavities, whose inferred ages are $\geq 10^8 \text{ yrs}$ in the outer regions

of Perseus (Nulsen et al. 2005). The inclusion of magnetic fields in bubbles which are inflated by kinetic-dominated jets seems to alleviate this problem (Robinson et al. 2004, Ruszkowski et al. 2007), but also reduce the extent to which the interior of the hot bubbles couple to the surrounding medium, making it much more difficult for AGN heating to balance cooling (e.g., Bruggen et al. 2009). Even when the bubbles are inflated by magnetically-dominated jets (Nakamura et al. 2007, Liu et al. 2008), they rise through the cluster ICM as bipolar structures, and it is unclear how they couple with the surrounding medium and distribute heating.

In this work, we discuss another aspect of these questions through an examination of a supplementary stellar source of energy and momentum injection. We assume that gas infall into a central cluster galaxy triggers star formation and consequently SNe explosions that produce turbulence. SNe-driven turbulence in galaxy haloes is quite a common phenomenon (see de Avillez 2000; de Gouveia Dal Pino et al. 2009 for reviews). Edge-on star forming galaxies often exhibit hot halos with structures that resemble chimneys and fountains extending for several kpc above the galaxy. Numerical simulations indicate that they are produced by SNe, which blow superbubbles that carve the disk material and propels gas outwards (Melioli et al. 2008; 2009 and references therein). Halo cloud complexes and filaments resulting from these processes are observed in star forming disk galaxies (e.g. Dettmar 2005). The role of SN-powered galactic winds in preventing central gas cooling has been also recently investigated in the context of fossil group of galaxies (Dupke et al. 2009).

This study explores the role of turbulence injected in the central region of NGC 1275. Our model examines the importance of turbulence in the suppressing the cooling flow, providing energy/momentum for the production of the complex filamentary structures of cold gas, and dragging magnetic energy outwards into the ICM. To this end we made magnetohydrodynamical (MHD) numerical simulations of turbulence evolution in a realistic distribution of cluster gas, threaded by a weak magnetic field. The model and initial setup of the simulations are described in the following section. The main results and discussions are presented in §3, and we draw our conclusions in §4.

2. The model

In order to simulate the role of turbulence on mass and energy feedback in a galaxy cluster core, we performed MHD simulations accounting for the hot gas surrounding the core galaxy, and introduced the turbulent energy injection at the central core that could represent the feedback from SNe in an ongoing starburst. The model was implemented in a well-tested Godunov-MHD scheme, in which we integrate the full set of MHD equations in conservative form (Falceta-Gonçalves, Kowal & Lazarian 2008, Burkhart et al. 2009, Kowal et al. 2009, Leão et al. 2009).

An external force term, $\mathbf{f} = \mathbf{f}_{\text{turb}} + \mathbf{f}_{\text{grav}}$, which is responsible for the turbulence injection and gravity, is explicitly incorporated into the momentum equation. The turbulence is introduced by a random solenoidal function in Fourier space within a

chosen range of scales (see Alvelius 1999 for details). The effects of radiative cooling are treated separately, as we compute $\frac{\partial P}{\partial t} = (1 - \gamma)n^2\Lambda(T)$, after each timestep, where n is the number density and $\Lambda(T)$ is the interpolation function from an electron cooling efficiency table for an optically thin gas (Gnat & Sternberg 2007).

The external gravity is introduced through an appropriately scaled fixed distribution of dark matter following the NFW profile (Navarro, Frenk & White 1996),

$$\rho_{\text{DM}}(r) = \frac{\rho_s}{(r/r_s)(1 + r/r_s)^2}, \quad (1)$$

where r_s represents the characteristic radius of the cluster and $\rho_s = M_s/(4\pi r_s^3)$. From isothermal pressure equilibrium the gas density may be described by $\rho(r) = \rho_0[\cosh(r/r_s)]^{-1}$. As initial setup for the simulations we used an initial core density $\rho_0 = 5 \times 10^{-2} \text{cm}^{-3}$ and $r_s = 30$ kpc, which results in a similar profile to the empirical density distribution (Sanders et al. 2004). The core temperature is set as $T_0 = 7 \times 10^7 \text{K}$ which gives a free-free cooling timescale of $\sim 400 \text{Myr}$. The turbulence is introduced within the range $1 < l_{\text{inj}} < 3$ kpc. This range of values is a little large - due to limited resolution - when compared to the typical sizes of galactic superbubbles inflated by starbursts, which are of the order of several hundreds of parsecs. The injection scales, however, do not play a major influence on the subject of this study. The turbulent energy injection occurs within a radius of 5 kpc around the core center, and is set at a constant rate of $P_{\text{inj}} = 10^{56} \text{erg Myr}^{-1}$. This value represents injection from 10^{-1}SNe/yr , in agreement with the expected value for NGC 1275 where the star formation rate is $\sim 30 M_{\odot} \text{yr}^{-1}$ (Dixon et al. 1996).

Faraday rotation and synchrotron measurements obtained for several galaxy clusters have suggested magnetic field intensities of $B \sim 0.1 - 1 \mu\text{G}$, for the cluster halo. In our simulations, the magnetic field is assumed to be initially uniform in the x-direction, with intensity $B_0 = 1 \mu\text{G}$, very small compared to the thermal pressure ($\beta \sim 10^4$) but in agreement with the observations. Because of the high beta value the initial topology of the field is dynamically irrelevant. The computational domain corresponds to a box with physical size of $L = 100$ kpc. The cube is homogeneously divided into fixed 256^3 cells, corresponding to 0.39 kpc/cell. We have also used open boundary conditions in order to allow gas motions in/outward the computational domain as the pressure gradients evolve with time.

3. Results

The simulations were carried out over a time span of $t = 150$ Myr, consistent with the extended period of star formation in NGC1275 based on ages of its massive star clusters (e.g. Carlson et al. 1998). Turbulence is initially responsible for small (low density) bubbles. At the same time, as the gas starts to cool, there is an inward flux as a cooling flow. At this stage, the small cavities do not expand much since the shock heating is efficient only in the core region where the sound speeds are small. As the distance to the center of the system increases the sound speed increases and

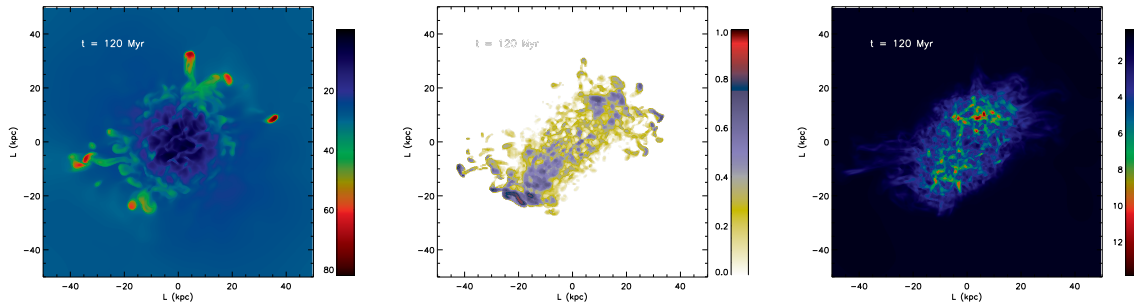


Figure 1. *Left:* 2D slice of map of density normalized by local density at $t=0$. *Center:* Emission map for the overdense filamentary structures normalized by a maximum value (see text). *Right:* projection of magnetic pressure ratio ($\int_{LOS}(B^2/B_0^2)dl/L$).

shock dissipation becomes less efficient. However, as more turbulent cells are randomly injected, eventually coinciding with previously inflated cavities, further expansion is observed.

The interaction between the SN-driven turbulence and the overdense structures results in the formation of the gaseous filamentary structures, as shown in Figure 1 (left) at $t = 120$ Myr. The map of overdense structures was obtained by dividing the density map of the central slice of the cube at $t = 120$ Myr by its value at $t = 0$ Myr. In Figure 1 (center) we show the emission map for a given line of sight, assuming the gas is optically thin. For this plot we considered the emission (which is proportional to the density squared) from the densest regions, above an arbitrary threshold taken as 5 times the averaged density. The contribution from cells below this threshold was set to zero. This calculation mimics the optical emission from molecular gas, which occurs only at the densest regions. The filaments have sizes of ≤ 40 kpc, and move outward with average velocities of $\sim 100 - 500$ km s $^{-1}$. At the end, ram pressure exerted by the outward turbulent motion counter-balances the incoming cooling flow; matter infall ceases at $t \sim 10$ Myr.

During the formation of the filaments, the magnetic field is dragged and compressed with the gas. The local density within the filaments is $n \sim 0.01 - 0.04$ cm $^{-3}$, a factor of $\sim 10 - 100$ times larger than the ambient value. As a result, the magnetic pressure within the overdense filaments and loops is typically larger than the surroundings by a factor of $30 - 200$, i.e. the filaments present absolute values of magnetic field intensities in the range $B_{fil} = 5 - 20 \mu\text{G}$ (as seen in Fig. 1 [right]). This value is comparable to the estimation of $B \sim 24 \mu\text{G}$ (Fabian et al. 2008) based on stability conditions for gravitational support. The surroundings, on the other hand, present field intensities in the range $0.1 - 1 \mu\text{G}$, in agreement with synchrotron and Faraday rotation estimates (Carilli & Taylor 2002). A strong magnetic field would also be responsible for a decrease in gas diffusion and thermal conductivity, which would allow the filaments to further decrease in size and increase in density due to cooling (Revaz et al. 2008). Higher gas densities in the filaments are required to match the observations.

Another important feature observed in the simulation is the generation and

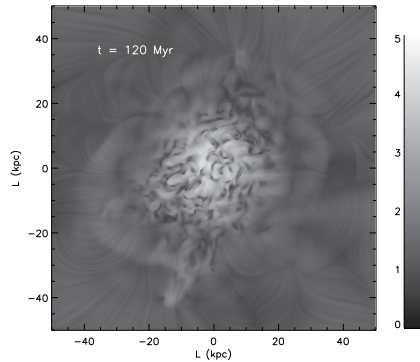


Figure 2. Line integral convolution map for the velocity field using the same time step as in Fig. 1 ($t = 120$ Myr). Gray-scales correspond to velocity amplitudes which are related to the local sound speed (Mach number) and texture corresponds to vectors orientation. Spherical shaped shock fronts propagate outwards in different directions.

propagation of acoustic waves. Fabian et al. (2003) studied the excess emission in X-rays from Chandra observations and identified weak shock fronts, or acoustic waves, propagating outwards the inner part of Perseus. Figure 2 presents the two dimensional line integration convolution method (LIC) applied to the velocity field of the middle slice of the simulated cube. The texture of the plot represents the orientation of the velocity vectors, and the gray-scales represent its local intensity relative to the sound speed (bright regions in the center show the turbulence injection scales). The shell-like gradients in gray-scales represent the acoustic waves, or even shocks, if present, propagating outwards as seen in the observations. Fabian et al. (2003) have speculated about their origin considering the effects of rising bubbles inflated by the AGN. The isotropic distribution of the ripples and weak shocks indicates that they may be well explained by the turbulence itself.

In spite of allowing the formation of loops and dense filamentary structures, as well as the increase of magnetic field intensity within ripples and filaments, and the generation of nearly isotropic shock/acoustic waves, turbulence alone cannot be responsible for the heating of the central region of the cluster. Even though ICM infall ceases, mostly due to the isotropic momentum distribution of the turbulent motions, cooling still dominates. Being subsonic over most of the simulated volume, the turbulent kinetic energy is not efficiently converted into heat. Therefore, another heating source is required.

Actually, the AGN, although not providing much momentum to the gas, is the main source of energy in NGC 1275 (and possibly in most galaxy clusters). In order to test its importance in heating the cluster core, we performed a 2.5-D simulation with similar setup as described in the run above, but including an AGN “heavy” particles jet, i.e. of ions, with a total power of $L = 10^{43}$ erg s $^{-1}$. For that we use a standard procedure (*see* Heinz et al. 2006), selecting 2 cells in the center of the simulated domain and fixing the local velocity as $v_{\text{jet}} = 20c_s$ (which corresponds to $\sim 10^4$ kms $^{-1}$) in both opposite directions along the x-axis. The jet temperature is set as $T_{\text{jet}} = 10T_0$, and its density as

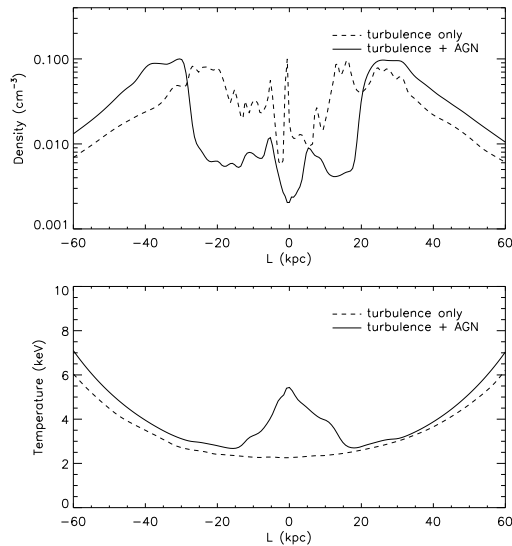


Figure 3. Density (top) and temperature (bottom) profiles as obtained for a 2.5 D turbulent model without AGN heating (solid line) and turbulence plus AGN heating model (dashed line).

$n_{\text{jet}} = 0.1n_0$, resulting in a total mass loss rate of $\sim 0.2M_{\odot}\text{yr}^{-1}$.

In Figure 3, we compare the average radial temperature profiles obtained for each model, i.e. with and without the inclusion of the AGN. The AGN represents the main source of heating in the system, but turbulence is still required to *isotropize* its distribution. It is important to remark that, though we do not show the maps here, the density structures, as observed in the slices of the 3-dimensional MHD turbulence discussed above, are almost the same in the model including the AGN. This follows because the AGN momentum is much smaller than that injected by the SN-driven turbulence.

4. Conclusions

In this work we presented a study of the role of MHD turbulence in the formation of large scale density structures in the central regions of galaxy clusters with the objective of better understanding the giant gas filaments in NGC 1275. Since AGNs do not seem to provide enough momentum to distribute their power isotropically around the cluster core, they may not be the main mechanisms responsible for filamentary and shell-like ISM structures found, e.g., in the Perseus galaxy cluster. Our model provides additional energy/momentum to the intracluster plasma via SNe explosions which we relate to the high star formation rate in NGC 1275. These can produce shocks that propagate outwards, pushing enough of the ISM to qualitatively reproduce the observations.

Our numerical simulations of MHD turbulence injected in a realistic ICM have shown that most of the peculiar structures observed in NGC 1275 might be reproduced if a SNe injection power of 10^{56} erg Myr $^{-1}$ (typical for starburst galaxies) is used. This

process raises gas loops and filaments with average velocities of $\sim 100 - 500 \text{ km s}^{-1}$, compatible with the observations. Some filaments are related to bubble motions. This is not surprising as the turbulence itself results in the creation of small scaled bubbles that evolve being dragged outwards. Compared to AGN inflated bubble models, though, our model results in more isotropic distributions and presents shorter evolutionary timescales. These structures are also threaded by magnetic fields whose intensity is amplified by compression. In order to verify this possibility we have calculated the B versus n correlation. For the filaments we obtained $B \propto n^{0.87}$. The power index, close to unity, is expected for magnetic compression at shocks. Magnetic fluctuations due to MHD waves, on the other hand, result in power index close to 0.5, which is comparable to the value 0.41 obtained for the halo, disregarding the filaments. The resulting magnetic pressure is similar to the required values of $\sim 25 \mu\text{G}$ to help stabilize them against gravitational collapse and diffusion, while the magnetic field at the halo is kept in the range $0.1 - 1 \mu\text{G}$. The major role of the magnetic field is to stabilize the filamentary structures. For example, magnetic field reduced the effect of Kelvin-Helmholtz instability at the edge of the structures and helped preventing the diffusion of the cooled material with the surroundings. Of course, the transport issue is quite important to address (see e.g., Parrish, Quataert & Sharma 2009), though it has not been calculated in our models. However, as pointed by Dennis & Chandran (2005), the energy transfer rate by heat conduction is very small compared to the dynamical sources. Because of the isotropic momentum injection, the ICM infall due to the cooling flow is ceased at $t \sim 10 \text{ Myr}$. However, the temperature at the core is not increased, as expected from the observations. This is an indication that turbulence may be the main source of momentum to the system, but not the main heating source. From 2.5-D simulations of MHD turbulence working together with a typical AGN of $L = 10^{42} \text{ erg s}^{-1}$, we also reproduced the radial temperature profile observed in NGC 1275.

Our results have special importance for understanding the halting of cooling flows in galaxy clusters. AGN may provide enough energy for the heating of the cooled gas in the cluster cores, but turbulence - even though not necessarily related to starbursts - is needed to isotropize and distribute the energy. A more detailed analysis, including fully 3-dimensional modeling also with AGN heating, as well as models with finer resolution, is currently in process and will be presented in a future work.

The authors acknowledge support from FAPESP and CNPq grants. JSG received support from NSF grant AST-0708967 to the University of Wisconsin.

- [1] Alvelius K. 1999, *Phys. Fluids*, 11, 7, 1880
- [2] Bruggen M., Ruszkowski M. & Hallman E. 2005, *ApJ*, 630, 740
- [3] Bruggen M., Scannapieco E. & Heinz S. 2009, *MNRAS*, 395, 2210
- [4] Burkhart, B.; Falceta-Gonçalves, D., Kowal, G., Lazarian, A. 2009, *ApJ*, 693, 250
- [5] Carilli C. L. & Taylor, G. B. 2002, *ARA&A*, 40, 319
- [6] Carlson M. N. et al. 1998, *AJ*, 115, 1778
- [7] Conselice C. J., Gallagher J. S. & Wyse R. F. G. 2001, *ApJ*, 211, 135
- [8] de Avillez, M. 2000, *MNRAS*, 315, 479

- [9] de Gouveia Dal Pino E. M., Melioli C., D'Ercole A., Brighenti F. C. & Raga A. 2009, *Adv. Space Res.*, in press
- [10] Dennis T. J. & Chandran B. D. G. 2005, *ApJ*, 622, 205
- [11] Dettmar R.-J. & Soida M. 2006, *Ast. Nachrichten*, 327, 495
- [12] Dixon, W. V. D., Davidsen, A. F., & Ferguson, H. C. 1996, *AJ*, 111, 130
- [13] Dupke R., Mendes de Oliveira C. & Sodré L. 2009, *ApJ* (submitted)
- [14] Fabian, A.C., Sanders J. S., Allen S. W. et al. 2003, *MNRAS*, 344, 43
- [15] Fabian, A.C., Sanders J. S., Taylor G. B. et al. 2006, *MNRAS*, 366, 417
- [16] Fabian A. C., Johnstone R. M., Sanders J. S. et al. 2008, *Nature*, 454, 968
- [17] Falceta-Gonçalves D., Lazarian A. & Kowal G. 2008, *ApJ*, 679, 537
- [18] Ferland, G. J., Fabian, A. C., Hatch, N. A. et al. 2008, *MNRAS*, 386, 72
- [19] Gardini A. 2007, *A&A*, 464, 143
- [20] Gnat O. & Sternberg A. 2007, *ApJ*, 168, 213
- [21] Godon, P., Soker, N., & White, R. E., III 1998, *AJ*, 116, 37
- [22] Graham J., Fabian A. C. & Sanders J. S. 2008, *MNRAS*, 386, 278
- [23] Hatch, N. A., Crawford, C. S., Johnstone, R. M., & Fabian, A. C. 2006, *MNRAS*, 367, 433
- [24] Heinz S., Bruggen M., Young A. & Levesque E. 2006, *MNRAS*, 373, 65
- [25] Johnstone R. M., Hatch N. A., Ferland G. J. et al. 2007, *MNRAS*, 382, 1246
- [26] Kowal, G., Lazarian A., Vishniac E., & Otmianowska-Mazur, K. 2009, *ApJ*, 700, 63
- [27] Leão, M. R. M., de Gouveia Dal Pino, E. M., Falceta-Gonçalves, D., Melioli, C., Geraissate, F. 2009, *MNRAS*, 394, 157
- [28] Liu W., Li H., Li S. & Hau S. 2008, *ApJ*, 684, 57
- [29] Melioli C., Brighenti, F. C., D'Ercole, A. & de Gouveia Dal Pino, E. M. 2008, *MNRAS*, 388, 573
- [30] Melioli C., Brighenti, F. C., D'Ercole, A. & de Gouveia Dal Pino, E. M. 2009, *MNRAS*, 399, 1089
- [31] Nakamura M., Li H. & Li S. 2007, *ApJ*, 656, 721
- [32] Navarro J. F., Frenk C. S. & White S. D. M. 1996, *ApJ*, 462, 563
- [33] Nulsen P. E. J., Hambrick D. C., McNamara B. R., et al. 2005, *ApJ*, 625, 9
- [34] Parrish I. J., Quataert E. & Sharma P. 2009, *ApJ*, 703, 96
- [35] Pistinner, S., & Shaviv, G. 1995, *ApJL*, 446, L11
- [36] Pizzolato F., & Soker N. 2006, *MNRAS*, 371, 1835
- [37] Revaz Y., Combes F. & Salomé P. 2008, *A&A*, 477, 33
- [38] Robinson K., Dursi L. J., Ricker P. M. et al. 2004, *ApJ*, 601, 621
- [39] Ruszkowski M., Ensslin T. A., Bruggen M., et al. 2007, *MNRAS*, 378, 662
- [40] Salomé P., Combes F., Edge A. C. et al. 2006, *A&A*, 454, 437
- [41] Sanders J. S., Fabian A. C., Allen S. W. & Schmidt R. W. 2004, *MNRAS*, 349, 952
- [42] Sanders J. S. & Fabian A. C. 2007, *MNRAS*, 381, 1381